

Collision Cross Sections and Ion Mobility Separation of Fragment Ions from Complex N-Glycans

David J. Harvey,^{1,2} Yasunori Watanabe,^{2,3,4} Joel D. Allen,² Pauline Rudd,⁵ Kevin Pagel,^{6,7} Max Crispin,² Weston B. Struwe^{3,8}

¹Target Discovery Institute, Nuffield Department of Medicine, University of Oxford, Roosevelt Drive, Oxford, OX3 7FZ, UK

²Biological Sciences and the Institute for Life Sciences, University of Southampton, Southampton, SO17 1BJ, UK

³Oxford Glycobiology Institute, Department of Biochemistry, University of Oxford, South Parks Road, Oxford, OX1 3QU, UK

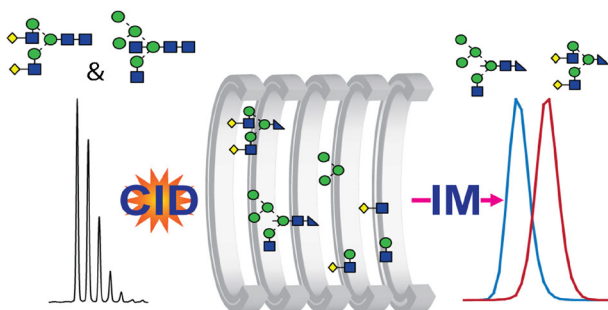
⁴Division of Structural Biology, University of Oxford, Wellcome Centre for Human Genetics, Roosevelt Drive, Oxford, OX3 7BN, UK

⁵NIBRT GlycoScience Group, The National Institute for Bioprocessing Research and Training, Dublin, Ireland

⁶Fritz Haber Institute of the Max Planck Society, Faradayweg 4-6, 14195, Berlin, Germany

⁷Institut für Chemie und Biochemie, Freien Universität Berlin, Takustrasse 3, 14195, Berlin, Germany

⁸Chemistry Research Laboratory, Department of Chemistry, University of Oxford, South Parks Road, Oxford, OX1 3TA, UK



Abstract. Ion mobility mass spectrometry (IM-MS) holds great potential for structural glycobiology, in particular in its ability to resolve glycan isomers. Generally, IM-MS has largely been applied to intact glycoconjugate ions with reports focusing on the separation of different adduct types. Here, we explore IM separation and report the collision cross section (CCS) of complex type N-glycans and their fragments in negative ion mode following collision-induced dis-

sociation (CID). CCSs of isomeric fragment ions were found, in some cases, to reveal structural details that were not present in CID spectra themselves. Many fragment ions were confirmed as possessing multiple structure, details of which could be obtained by comparing their drift time profiles to different glycans. By using fragmentation both before and after mobility separation, information was gathered on the fragmentation pathways producing some of the ions. These results help demonstrate the utility of IM and will contribute to the growing use of IM-MS for glycomics.

Keywords: Ion mobility, Complex N-glycans, Collision cross section, Glycomics

Received: 15 December 2017/Revised: 27 February 2018/Accepted: 27 February 2018/Published Online: 19 April 2018

Introduction

Ion mobility-mass spectrometry (IM-MS) is emerging as a powerful tool to interrogate glycoconjugates and is capable of differentiating isomeric structures [1–5]. IM-MS can improve glycan detection by its ability to separate glycans from many contaminating compounds whose ions display different collisional cross sections (CCSs) [6, 7] and fall on different CCS- m/z trend lines. Most examples of the technique reported to date

demonstrate separation of glycans arising from varied adduct formation [5, 8–11], ion polarity [10, 12, 13], methylation [14, 15], and reduction [16]. The separation of gas-phase ions by IM is driven by the size, shape, and charge of the analyte as it passes through a neutral gas, commonly nitrogen or helium, under the influence of a weak electric field. Properties that alter the three-dimensional structure of a glycan, such as fluorescent labelling, permethylation or the radius of a cation/anion adduct will, therefore, influence the drift time and the resulting arrival time distribution (ATD). The drift time is directly related to the CCS of a given carbohydrate ion, which is an intrinsic molecular property thus making its use for structural analysis universally applicable.

Glycan CCS values can be measured directly by drift tube (DT) instruments or by traveling wave (TW) instruments following calibration with compounds of known CCS values, such as dextran [17], analogous to glucose units in HPLC glycan analyses [18]. Glycan structural analysis by mass spectrometry is most easily accomplished by negative ion collision-induced dissociation (CID), which generates multiple cross-ring cleavage products diagnostic of specific structural features such as antenna branching and location of fucose residues [19–21]. Recently, IM separation of positive fragment ions has proven effective in discriminating anomeric and linkage information [22–25] as well as differentiating isomeric Lewis and blood group species [26]. Accordingly, combining IM and CID for glycomics holds tremendous potential, and here, we explore IM properties of complex type N-glycan standards and corresponding fragments as negative ions. We identify unique drift time properties of complex glycan fragments and show that isomeric structures can be identified by CID products in cases where identification by their parent ion precursors is difficult.

Experimental

Materials and Sample Preparation

Complex type N-glycan standards were purchased from Dextra Laboratories (Reading UK). Biantennary glycans containing fucose attached to their antennae were released with hydrazine from glycoproteins present in human parotid glands as described earlier [27]. Hybrid glycans ($\text{Glc}_1\text{Man}_4\text{GlcNAc}_3$ and $\text{Gal}_1\text{Man}_5\text{GlcNAc}_3$) were from the HIV glycoprotein, gp120 that had been produced in the presence of the α -mannosidase II inhibitor, swainsonine. The triantennary glycan, A3G3 (see Fig. 9 for structure and a description of the terminology used to describe glycan structures), branched on the 3-antenna was from bovine fetuin (Sigma) following desialylation by heating with 2% acetic acid for 30 min at 80 °C and the corresponding compound containing fucose attached to the 4-branch of the 3-antenna was obtained likewise from human α 1-acid glycoprotein (Sigma-Aldrich) [28]. The A2 glycan was released from chicken ovalbumin by hydrazinolysis followed by acetylation.

Samples were diluted with HPLC-grade water to a final concentration of 150 μM prior to use. One microliter from the stock solution was added to 8 μl 1:1 methanol/water (HPLC grade) and a trace amount of 100 μM ammonium phosphate solution to generate phosphate adducts (the adducts most commonly observed on samples from biological sources). Sample solutions were stored at -20 °C between analyses.

Ion Mobility-Mass Spectrometry

Traveling wave (TW) IM-MS measurements were performed on a Synapt G2Si instrument (Waters, Manchester,

UK). For each sample analysis, 2 μl of N-glycan stock material was ionized by nano-electrospray ionization (nano-ESI) from gold-coated borosilicate glass capillaries prepared in-house [29]. Instrument settings were as follows: capillary voltage 0.8–1.0 kV, sample cone 150 V, extraction cone 150 V, cone gas 40 l/h, source temperature 80 °C, trap collision voltage 4–160 V, transfer collision voltage 4 V, trap DC bias 60 V, IMS wave velocity, 450 m/s, IMS wave height 40 V, trap gas flow 2 ml/min, and IMS gas flow 80 ml/min. The vacuum pressures were as follows: backing = 3.3 mbar, source = $8.4e^{-3}$ mbar, trap = $2.4e^{-2}$, IMS = 2.8 mbar, and transfer = $2.7e^{-2}$. For investigating the origin of fragment ions from parent and primary fragments (later referred to as trap/transfer experiments), the first collision voltage (in the trap) was adjusted to a value where all relevant higher mass fragments were detected followed by a ramped secondary collision voltage (in the transfer) slowly over the range 30 to 110 V (higher voltages resulted in loss of the ion beam). Single ion plots of the target ions were then extracted from the accumulated data to identify their precursors. Data was acquired and processed with MassLynx v4.1 and Driftscope version 2.8 software (Waters, Manchester, UK). The nomenclature used to describe the fragment ions is that devised by Domon and Costello [30] with the addition of the use of the subscript R (for reducing terminus) to describe fragments of the reducing-terminal GlcNAc residue and R-1 to describe fragments from the other core GlcNAc. This nomenclature simplifies description of the fragmentation processes because it avoids the subscript number changing with different antenna chain lengths. An ion, named ion D, formed by loss of the chitobiose core and 3-antenna defines the composition of the 6-antenna.

TW-IM-MS and Collision Cross Section Estimation

Arrival time distributions (ATDs) of parent and product ions were fitted to a single or greater Gaussian distribution depending on the presence of single or multiple ATDs [31]. A dextran calibration ladder with known absolute drift tube $^{\text{DT}}$ CCS was used for estimating N-glycan $^{\text{TW}}$ CCS values as previously described [17, 32]. In brief, measured drift times (t_D) were corrected for m/z dependent delay time from Eq. (1) where c is an empirically determined constant ($c = 0.001 \times \text{EDC}$ (enhanced duty cycle) delay coefficient).

$$t'_D = t_D - c\sqrt{m/z} \quad (1)$$

Absolute dextran $^{\text{DT}}$ CCS was corrected for charge (z) and reduced mass (μ) of the ion and the drift gas (Eq. (2)).

$$\text{CCS}' = {}^{\text{DT}}\text{CCS} / \left[z \times \left(\frac{1}{\mu} \right)^{\frac{1}{2}} \right] \quad (2)$$

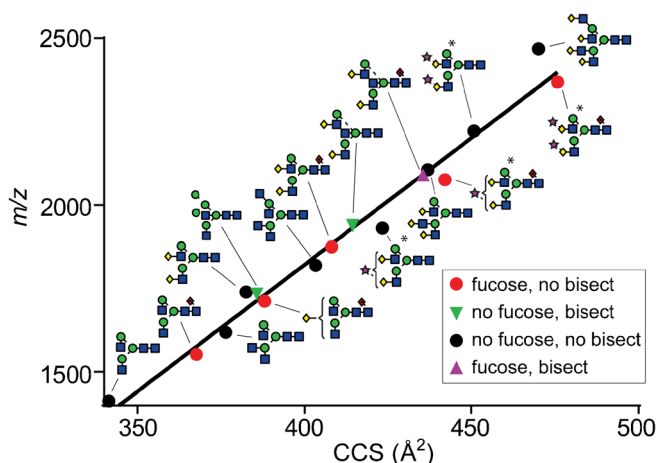


Figure 1. Plot of m/z against CCS for complex type N-glycans ions. All ions excluding sialylated structures (marked with an asterisk) were measured as singly charged phosphate adducts

A correlation plot of $\ln(\text{CCS}')$ versus $\ln(t_D')$ ($R^2 > 0.99$) gives two constants termed the fit-determined constant A and the slope X from the equation:

$$\ln \text{CCS}' = X \times \ln t_D' + \ln A \quad (3)$$

Estimated $^{\text{TW}}\text{CCS}$ values were then determined from experimental drift times by Eq. (4), derived from combining Eqs. (2) and (3) ($^{\text{DT}}\text{CCS}$ now replaced with $^{\text{TW}}\text{CCS}$):

$$^{\text{TW}}\text{CCS} = A \times z \times t_D'^X \times \left(\frac{1}{\mu}\right)^{\frac{1}{2}} \quad (4)$$

Sample preparation and MS reporting are in accordance with MIRAGE guidelines as described [33, 34].

Results and Discussion

IM separation of one hybrid and 13 complex type N-glycans were assessed using a traveling wave ion mobility instrument with nitrogen as the drift gas. The glycans included bi-, tri-, and tetra-antennary structures with core fucose ($n = 6$), bisecting *N*-acetylglucosamine (GlcNAc) ($n = 3$), and terminal sialic acid residues (*N*-acetylneuraminic acid; Neu5Ac) ($n = 4$). Collision cross sections of neutral (non-sialylated) glycans were measured as phosphate adducts due to the observation that phosphate, along with several other anions such as chloride and bromide, acts to stabilize neutral glycans during negative ionization and are the most common adducts found in glycans found in biological samples. Furthermore phosphate adducts do not have multiple isotopes, as is the case with chloride or bromide adducts [19] which may complicate interpretation of IM results. Sialylated N-glycan parent ions were measured as deprotonated species due to proton loss from carboxyl groups ($\text{pK}_a = 2.6$) in solution. However, all CID products of both sialylated glycans and phosphate anion adducts were

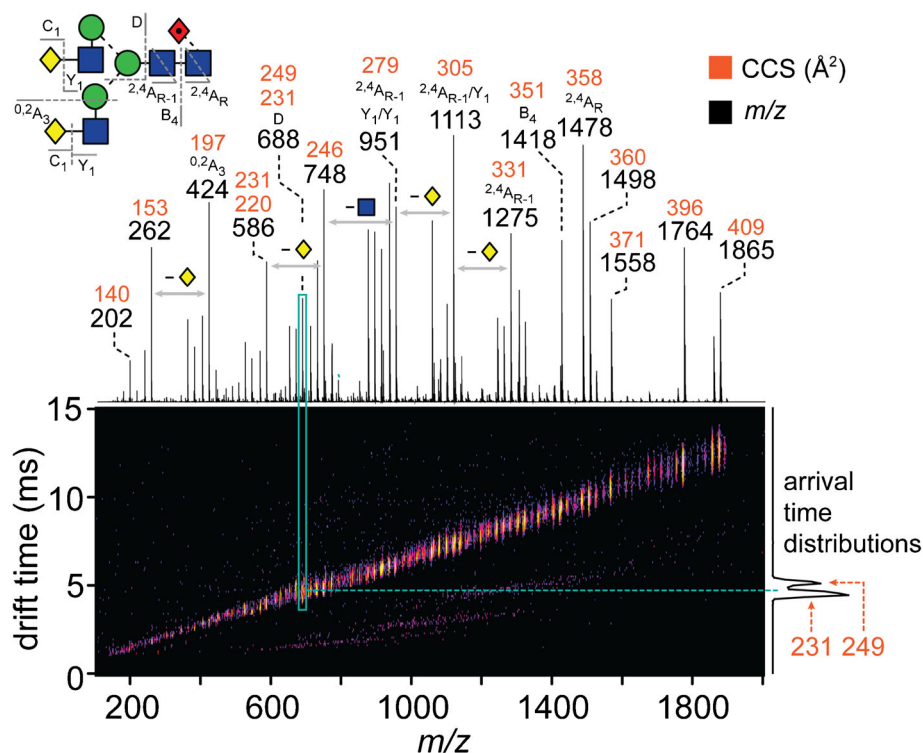


Figure 2. IM-MS/MS spectra (trap fragmentation) of the F(6)A2G2 glycan with corresponding CID spectrum above the IM drift plot. $^{\text{TW}}\text{CCS}_{\text{N}_2}$ are shown in orange, and m/z and corresponding fragmentation assignments are in black over each peak. The extracted ATD of the 1275 m/z ion is shown as representative data

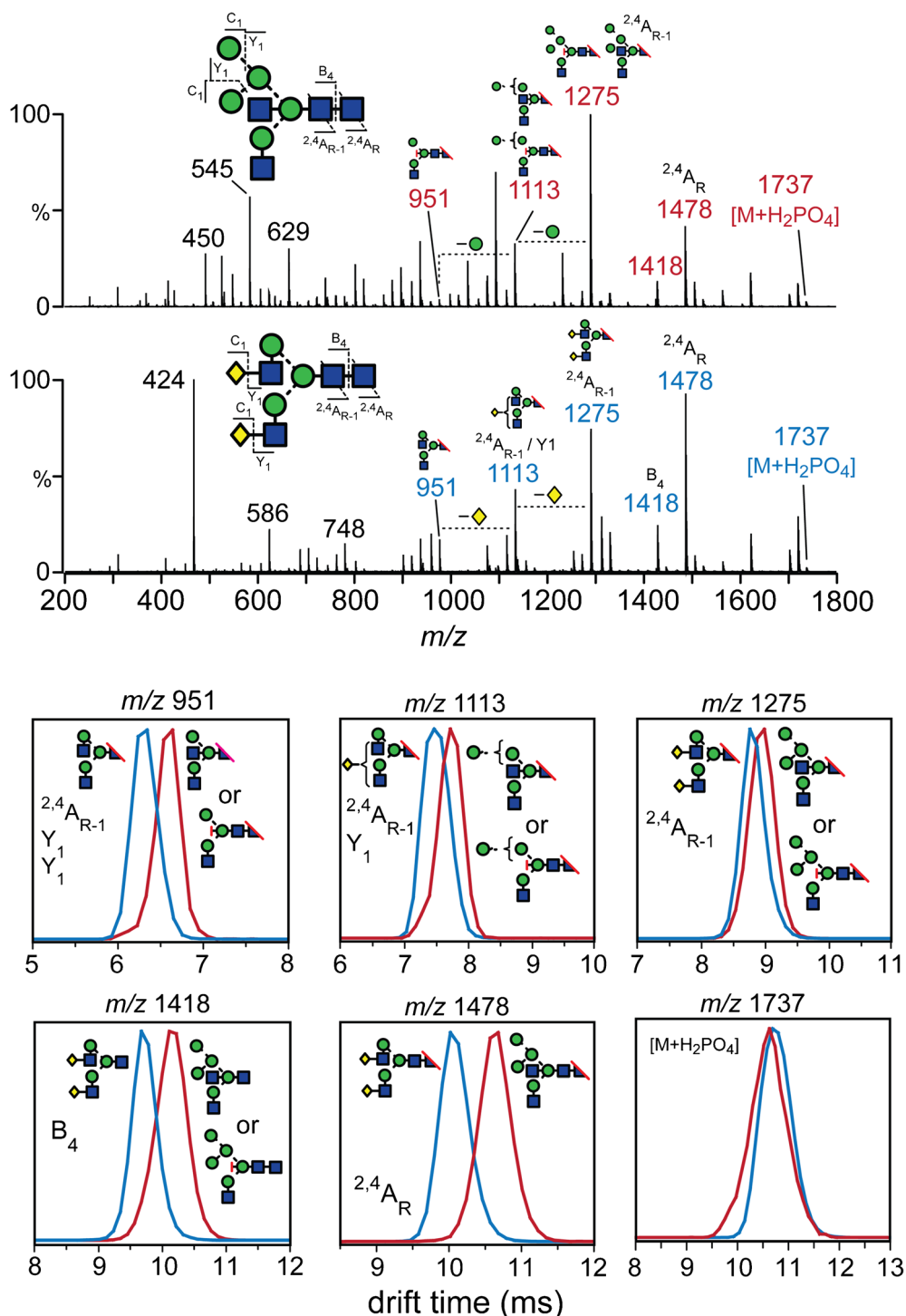


Figure 3. IM-MS/MS of hybrid bisect (HB) and A2G2 isomeric N-glycans (top). ATDs of fragment ions m/z 951, 1113, 1275, 1418, 1478, and 1737 parent ions (ions from A2G2 are shown in blue and HB are shown in red) (bottom). The red line on glycan structures of the ATD plots denotes the location of cross-ring fragments

deprotonated ions following loss of a proton or H_3PO_4 , respectively, as opposed to positive mode analysis where the cation adduct is generally retained with the product ions. Therefore, all CID IM measurements were performed on $[\text{M}-\text{H}]^-$ ions in this report.

General Correlations Between CCS Values and Structure

CCS values of parent $[\text{M} + \text{H}_2\text{PO}_4]^-$ ions ranged from 368 \AA^2 (bi-antennary, fucosylated; F(6)A2) to 476 \AA^2 (di-sialylated,

bi-antennary, fucosylated; F(6)A2G2S2). CCS values were plotted against m/z for each glycan with a linear regression line shown to relate IM to glycan mass data (Fig. 1). Non-sialylated, fucosylated glycans with zero, one, and two galactose residues were on the same trend line consistent with earlier reports of similar glycans derived from glycoproteins [35]. Correspondingly, the non-fucosylated, bi-antennary, di-galactosylated glycan A2G2, which has a similar m/z to that of the fucosylated A2G1 glycan (A2G2 minus a single galactose), had a reduced CCS. This trend for core-fucosylated glycans to have an increased CCS, as compared with their non-fucosylated counterparts, was also demonstrated by the two bisected glycans F(6)A2G2B and A2G2B. The CCCs of the sialylated glycans generally fell below the trend line showing an increase in relative CCS for both mono-sialylated and one of the bi-sialylated glycans (F(6)A2G2S1) but not the equivalent glycan lacking fucose (A2G2S2). The rationale for this observation is difficult to predict, as modeling gas-phase $[M-H]^-$ glycan ions is exceedingly challenging, evident from previous attempts using quantum mechanical and ab initio molecular dynamics simulations [33]. However, these calculations were based on neutral oligosaccharides (i.e., non-sialylated), and to the best of our knowledge, molecular dynamics (MD) has not been performed on sialylated glycans. Lastly, the CCS of the tetra-antennary A4G4 glycan did not align with other structures and appears to adopt a more compact gas-phase conformation.

Overall, the use of CCS values to characterize glycan structures is helpful, but employing IM to discern glycan isomers on their intact properties alone (i.e., glycan plus adduct) is not always sufficient because of limited resolution of current commercial instruments. Consequently, the use of IM drift properties of lower mass fragment ions for differentiating glycan isomers was investigated.

Information from Fragment Ions

Glycan fragment ATDs are highly informative, and IM has previously proven capable of establishing oligosaccharide topology, linkage, and anomeric configuration information [12, 22]. Structural features, specifically terminal fucose linkage (i.e., blood group and Lewis epitopes), can be identified by IM when examining fragment ATDs and CCSs [26]. This can be done by IM separation following CID dissociation (generated in the trap region of a Synapt instrument), illustrated in Fig. 2 with the fucosylated biantennary glycan F(6)A2G2. These data often contain extensive diagnostic information that is efficient at discriminating between isomeric glycan structures even in cases where MS/MS results or CCS of parent ions cannot. An example is m/z 688, which can differentiate between the two antennae of the F(6)A2G2 biantennary glycan as discussed below.

An example of two N-glycan isomers with similar parent ion CCSs but different fragment CCSs is the biantennary (A2G2) and hybrid, bisecting (HB) glycans (m/z of 1737, Fig. 3). The

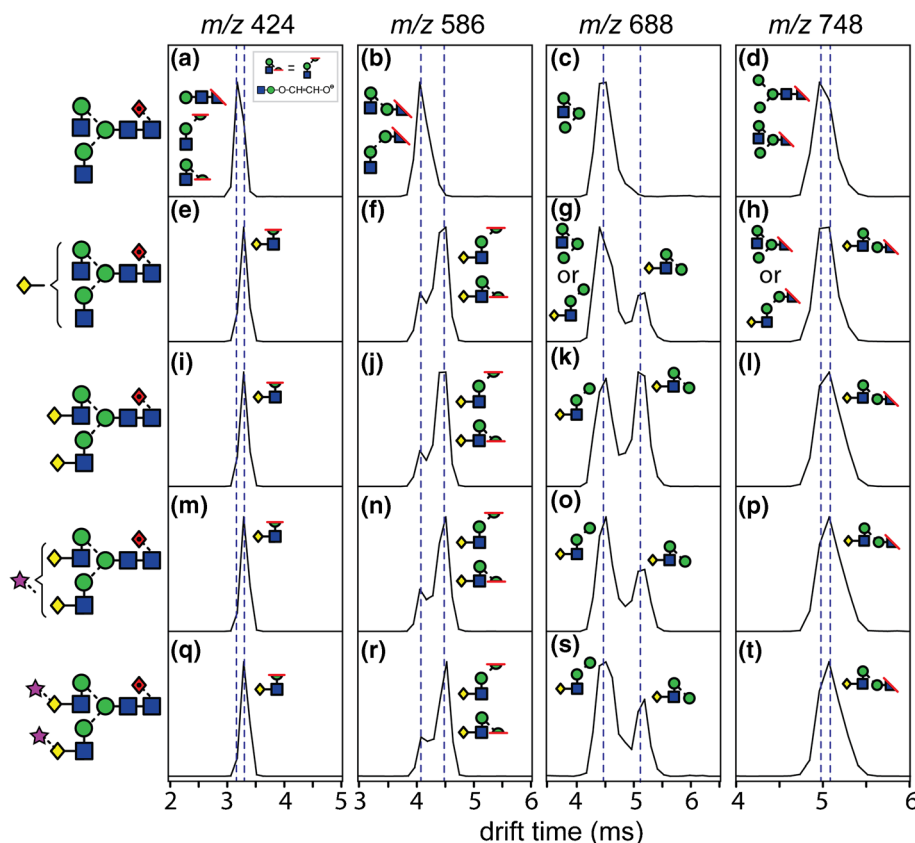
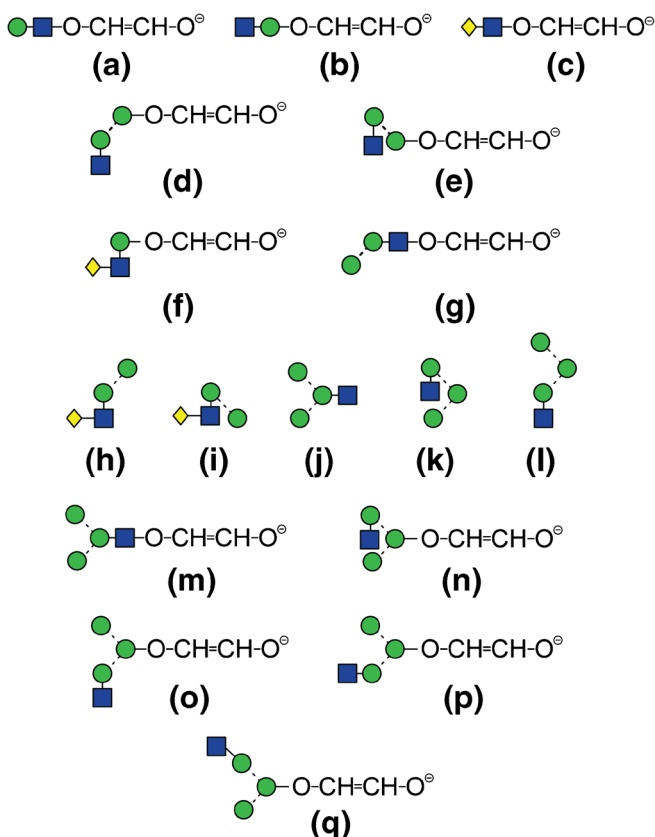


Figure 4. ATDs of cross-ring and D-type fragments m/z 424, 586, 687, and 748 from bi-antennary N-glycans F(6)A2, F(6)A2G1, F(6)A2G2, F(6)A2G2S1, and F(6)A2G2S2. The location of cross-ring fragmentation is shown as a red line



Scheme 1. Structures of N-glycan fragments. Structures of N-glycan fragments

CCSs of both intact glycans differ by $< 1\%$ (383 and 386 \AA^2 for A2G2 and HB, respectively). The MS/MS spectra of these glycans contain different fragments in the lower mass region, but the major ions from both compounds are the cross-ring $^{2,4}A$ -type fragments from the reducing (m/z 1478) and penultimate (m/z 1275) *N*-acetylglucosamine (GlcNAc) residues (shown on the glycan cartoon structures in Fig. 3). The ATDs of the m/z 1478

$^{2,4}A_{R-1}$ ions are notably different, yet the m/z 1275 $^{2,4}A_{R-1}$ ions are only slightly separated. It is important to note that the m/z 1275 ion could also arise from the loss of bisecting GlcNAc (shown) or 3-antennae GlcNAc from m/z 1478. However, because the diagnostic fragmentation for the presence of a bisect (m/z 629) is loss of the bisecting residue, the assignments of m/z 1418, 1275, 1113, and 951 have several possible origins, namely from the loss of the bisect and also neutral losses of the $^{2,4}A_{R-1}$ fragment as shown in Fig. 3. Interestingly, following the loss of a single hexose (m/z 1113) or two hexoses (m/z 951) from the m/z 1275 ion, the resulting ATDs of A2G2 and HB are separated. The additional Y-type cleavages from these ions are from the neutral loss of two mannose (Man) residues from the hybrid glycan, HB, and two galactose (Gal) residues from the biantennary glycan, A2G2. Lastly, the B-type fragments (m/z 1418) were also separated. Seemingly, the loss of bisecting GlcNAc has influence in the gas-phase conformations of deprotonated ions as opposed to phosphate adduct ions. Importantly, these results raise the possibility that the presence of bisecting GlcNAcs and subsequent loss of this residue during CID generate fragment structures that significantly differ from the equivalent mass fragment of the branched structure. If the primary fragment ions of m/z 1418, 1275, 1113, and 951 are from the loss of bisecting GlcNAc and not some type of $^{2,4}A_{R-1}$ plus respective neutral hexose loss, then penultimate GlcNAc on the core is retained and may be an important feature for IM separation of these fragments.

Another example where fragment IM is more informative than that of the intact N-glycans is from fucosylated biantennary structures with zero (F(6)A2), one galactose (F(6)A2G1), two galactose (F(6)A2G2) with one F(6)A2G2S1), and two (F(6)A2G2S2) sialic acids (Fig. 4). The two isomers of F(6)A2G1 (i.e., galactose linked to the 6- or 3- arm) have not yet been resolved by IM as phosphate adducts [35], but by evaluating deprotonated fragment ATDs, the linkages of the galactose residues can be verified from several fragment ions, namely m/z 424, 586, 688, and 748.

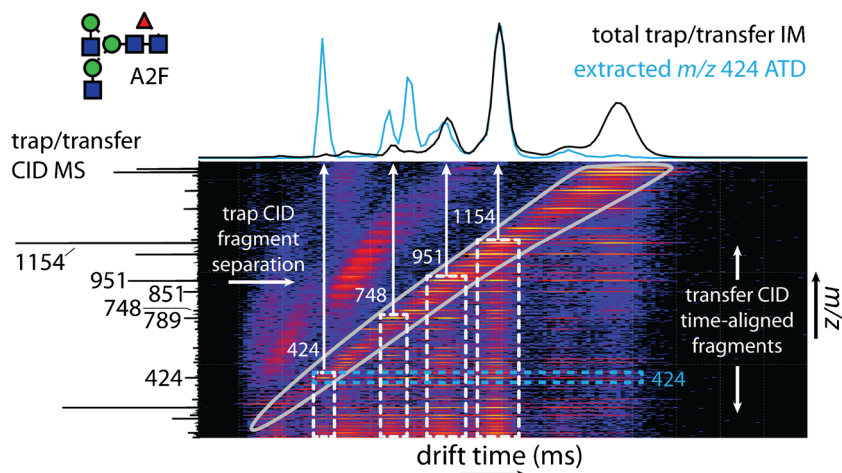


Figure 5. Simultaneous trap/transfer CID of the F(6)A2 glycan showing IM separation of trap CID ions (circled in gray) and transfer CID (time-aligned) fragments (white dotted lines). The extracted ATD of m/z 424 is shown in blue (top) as well as their location in the drift plot (blue dotted line). The trap/transfer ATD of all glycan fragment ions produced from both CID events is shown in black (top) and corresponding MS CID spectrum (left)

For the five fucosylated, biantennary glycans tested, m/z 424 fragment ion yielded a single ATD but with different drift times. The possible structures of the F(6)A2 glycan are varied, with two possible CID products corresponding to this mass (shown as structure **a** and **b** in Scheme 1). To identify the source of this fragment (i.e., which part of the precursor it was derived from following CID), we used a trap/transfer experiment, where the precursor is fragmented in the trap (prior to IM) with mild dissociation energy, followed by CID in the transfer region (post IM) producing a MS³ type of analysis. In this way, the fragments produced from the second (transfer) CID have the same drift times (i.e., time aligned) to their precursors. The data generated is shown in Fig. 5 and informs whether the m/z 424 originates

primarily from the molecular ion or diagnostic fragments generated during trap activation. These data showed that the m/z 424 was from m/z 1154 (^{2,4}A_R) and m/z 951 (^{2,4}A_{R-1}) indicating that both structures **a** and **b** were present as shown in Fig. 4 and probably accounting for the asymmetry of the m/z 424 ATD peak. The two possible cross-ring m/z 424 fragments of the core mannose from F(6)A2 are shown in Fig. 4a but are equal structures (**b**, Scheme 1). The corresponding ion from Man₃GlcNAc₂, which can only have structure **a**, aligned with the second component of this peak (data not shown). The ion at m/z 424 from the remaining galactosylated biantennary glycans (Fig. 4e, i, m, q) mainly has structure **c** (Scheme 1) and displays a slightly displaced ATD maximum from the peak from F(6)A2.

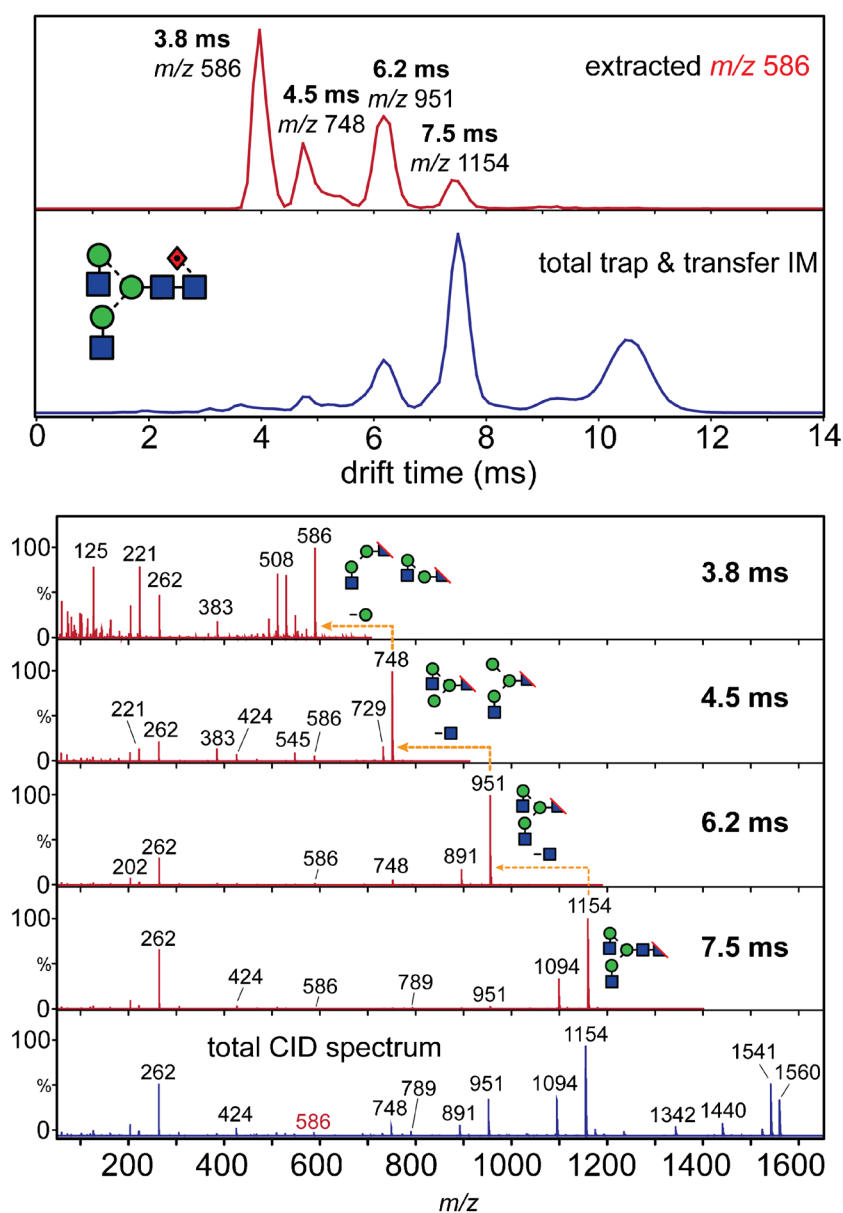


Figure 6. Trap/transfer extracted ATDs of the m/z 586 ion from F(6)A2. The ATD from all fragment ions is shown (blue chromatogram), and the four extracted ATDs of the m/z 586 ion are shown in the red chromatogram. The corresponding CID spectra of the m/z 586 ATDs are indicated (red) and the overall CID spectrum from the precursor F(6)A2 glycan (blue, bottom)

When evaluating the ATD of the m/z 586 ion (Hex₂GlcNAc₁ composition), the non-galactosylated F(6)A2 structure was found to have a single, broad ATD peak (Fig. 4b). A trap/transfer CID experiment was also used to establish the possible structures of this fragment. This spectrum displayed four peaks, the m/z 586 fragment (3.8 ms) from the molecular F(6)A2 ion, and three ATDs corresponding to m/z 1154 (^{2,4}A_R 7.5 ms), 951 (^{2,4}A_{R-1} 6.2 ms), and 748 (^{2,4}A_{R-1}-GlcNAc 4.5 ms) precursor fragment ions (Fig. 6). The major ATD arising from a fragment was from the ^{2,4}A_{R-1} ion ^{2,4}A_{R-1} at m/z 951 (6.2 ms drift time) supporting the structures **d** and **e** (Scheme 1). The galactosylated structures measured in Fig. 4f, j, n, r produced two ATDs, the first of which was coincident with the ATD from the F(6)A2 glycan (structures **d** and **e**). The second peak was produced by all of the galactosylated biantennary glycans and is a Gal-GlcNAc-O-CH=CH-O⁻ structure (ion **f**).

Two galactose-containing structures (**h**, **i**) are possible for the larger ion at m/z 688 (Hex₃GlcNAc₁) depending on which antenna they originate from and, indeed, two well-separated ATD peaks were observed from the biantennary glycans (Fig. 4g, k, o, s). However, other structures such as **j**–**l** in Scheme 1 are also possible. In order to determine which ions were responsible for the two observed peaks in Fig. 4, the ATD profiles of the equivalent ion from several other glycans were examined (Fig. 7). Man₃GlcNAc₂ (Fig. 7, green trace) should give only ion **j** and the ATD of m/z 688 from this compound aligned with the first of the peaks from the biantennary glycans discussed above. Similarly, the m/z 688 ion from the un-galactosyl biantennary F(6)A2 glycan (red trace, possible structures **k** and **l**) also aligned with the first of the biantennary glycan peaks showing that this peak could contain at least three structures. The second of the two peaks was only present in the spectra of glycans that contained non-fucosylated galactosylated 6-antenna, a situation that paralleled that of m/z 586, discussed above. This peak, therefore, must contain one or both of structures **h** and **i**. The spectra of the hybrid glycans, all of which contained the structure of ion **h**, produced an ATD peak (Fig. 7, blue trace) that coincided with the right hand side of the first of the peaks from the biantennary glycan. Thus, the drift time (or CCS) of the ion at m/z 688 can be used to characterize the two antennae. The conclusion that the second peak is produced by ion **i** is consistent with the observation that the triantennary glycan A3G3 produced only the second peak (light blue trace), and this observation, combined with the relatively small contribution of ion **h** to the first peak, supports the earlier conclusion that m/z 688 in these complex glycans is predominantly the D ion (ion **i**).

To complicate matters further regarding contributions to the structures forming m/z 688, the trap/transfer spectrum of the first of the biantennary peaks suggested additional formation from the cross-ring ^{2,4}A_{R-1} ion. Such an ion must have lost an equivalent mass (60 units) from another part of the molecule as that gained from the cross-ring fragment, leaving a residue of 102 mass units. Fragmentation of this ion showed that, indeed, the major fragment represented loss of 102 U, supporting such a double cross-ring structure. To conclude, therefore, the second of the two peaks from the biantennary glycans appeared to

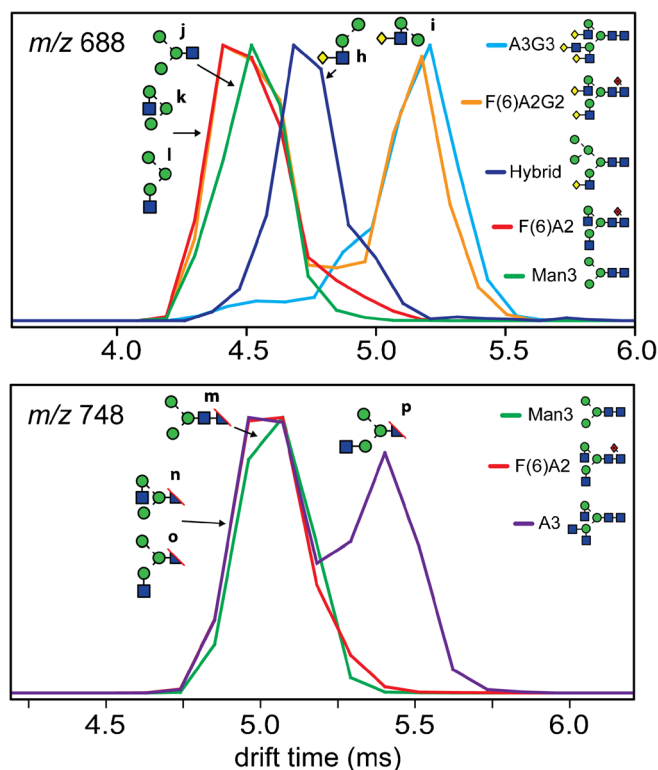


Figure 7. ATDs of the m/z 688 ion from Man₃GlcNAc₂ (Man3), F(6)A2G2, F(6)A2, and A3G3 glycans (top). ATDs of the m/z 748 ion from Man₃GlcNAc₂ (Man3), F(6)A2, and A3G3 glycans (bottom)

be ion **i** from the 6-antenna (the D ion), but the first peak appeared to be a complex mixture of structures, precluding the identification of a peak specific to the 3-antenna.

We next compared fragment ATDs from bi-, tri-, and tetra-antennary glycans with GlcNAc residues terminating the non-reducing end of the molecules. Characteristically, the major fragment ions in the MS/MS spectra were ^{2,4}A cross-ring fragments of the reducing and penultimate GlcNAc (chitobiose core) with additional Y-type cleavages of the terminal GlcNAc residues (Figs. 8 and 9). The ^{2,4}A_R fragment ATD (m/z 1560) from the tetra-antennary structure (A4) is a single distribution (blue chromatogram). The equivalent ions from the triantennary (m/z 1357, red trace) and bi-antennary (m/z 1154, green trace) glycan also displayed single ATDs. The m/z 1357 ion from the tetra-antennary glycan (A4) can be assigned to either the ^{2,4}A_{R-1} fragment or to the ^{2,4}A_R ion plus a neutral loss of one of the four non-reducing terminal GlcNAc residues (Y₄ cleavage). The extracted ATD showed a complex profile (blue trace) indicating the presence of several of these ions. Although non-linear Gaussian fitting could define the profile, the instrumental resolution was too low to determine if the calculated Gaussian peaks were reliable. Like the results for the tetra-antennary glycan, A4, the m/z 1154 ion from the triantennary glycan, A3, resulted in two well separated ATD distributions (red trace). The early peak aligned with the ^{2,4}A_R fragment from the bi-antennary F(6)A2 structure (green chromatogram) consistent with loss of the 4-linked galactose residue on the 3-

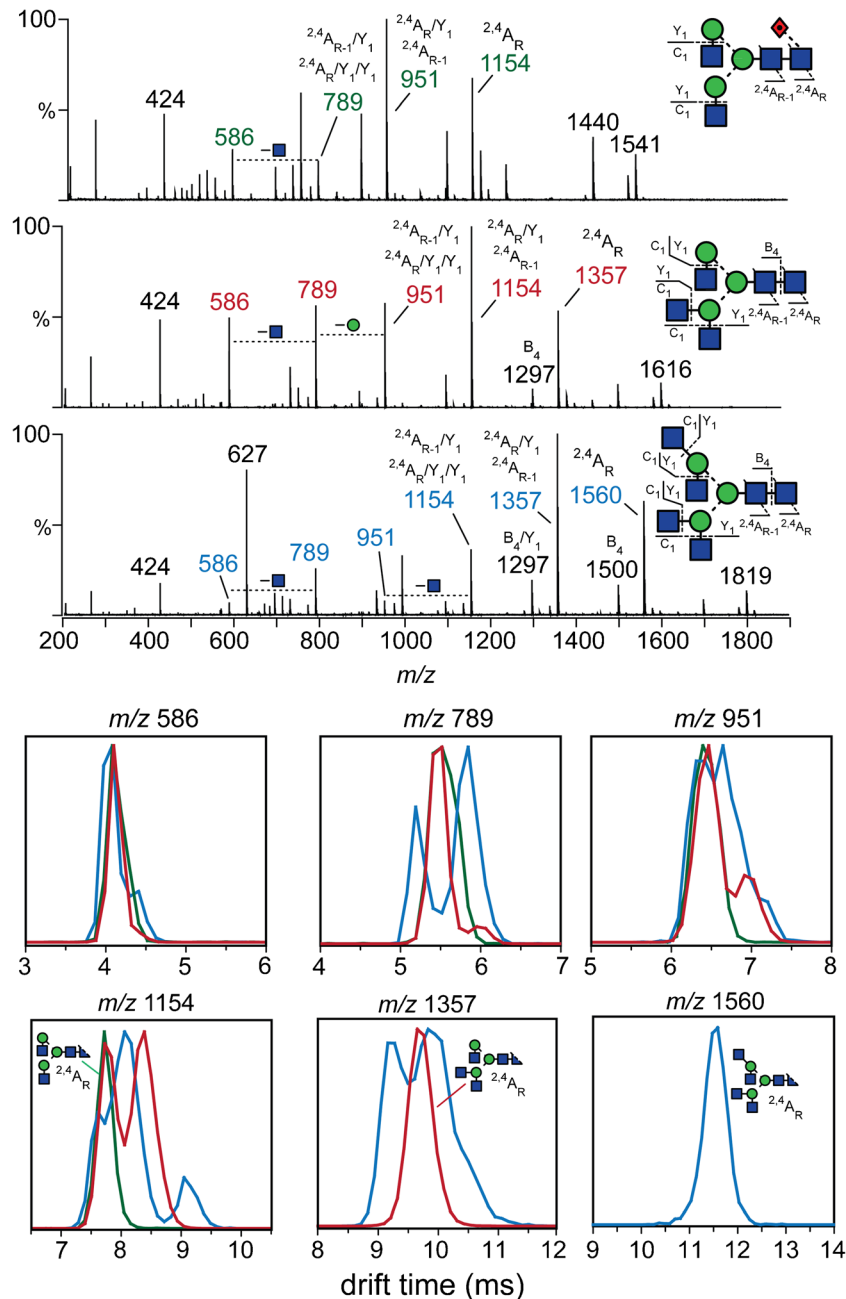
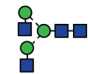
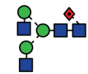
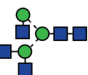
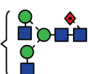


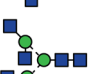

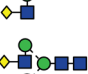
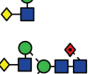
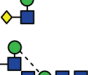

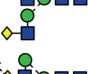






Figure 8. IM-MS/MS of bi-, tri-, and tetra-antennary N-glycans with terminal GlcNAc residues (top). ATDs of fragment ions m/z 586, 789, 951, 1154, 1357, and 1560 (F(6)A2 are green, A3 are red and A4 are shown in blue)


antenna. There were three distributions for this ion from A4 further highlighting the range of glycan fragments present in the MS/MS spectra arising from Y_4 fragments. The m/z 951 ion ($\text{Man}_3\text{GlcNAc}_2$ -containing ions) is from an additional GlcNAc loss from m/z 1154 and was observed as a single ATD for F(6)A2 (green trace), which could be derived from three fragments ($^{2,4}A_{R-1}$ or $^{2,4}A_R/Y_4$ (two ions)) as well as two and three ATDs for A3 and A4, respectively. The major ATD from A3 (red chromatogram) and the earliest A4 ATD align with the F(6)A2 peak suggesting similar glycan fragment structures. However, upon further loss of a single mannose (-162 Da, m/z 789), the resulting ATD of the A4 glycan (blue trace) differed further from that from A3 (red trace) and F(6)A2 (green


trace). Furthermore, following an additional GlcNAc loss (m/z 586), the ATDs were similar but not identical. Highly branched glycans, such as A4 and likely similar glycans with galactose and LacNAc extensions, pose a considerable challenge in the ability to assign ATDs to specific fragment structures. The possible combinatorial fragments from Y-fragments with $^{2,4}A_{R-1}$ or $^{2,4}A_R$ cleavages from the A4 glycan could result in five possible structures for m/z 1357 and up to 18 for the m/z 1154 fragment. Assigning ATD peaks is exceedingly challenging, and therefore, the best application may be in assessing IM of smaller fragments for glycan structural assignments.


Another ion showing isomeric separation was the cross-ring fragment m/z 748 ($\text{Man}_3\text{GlcNAc}_1$ plus $-\text{O}-\text{CH}=\text{CH}-\text{O}^-$). Five


structure	name	m/z [M+H ₂ PO ₄]	CCS (Å ²)
	A2	1413.5	341.5
	F(6)A2	1559.5	367.7
	A3	1616.5	376.5
	F(6)A2G1	1721.6	388.1
	A2G2	1737.6	382.6
	hybrid, bisect	1737.6	385.7
	A4	1819.6	403.3
	F(6)A2G2	1883.6	408.1
	A2G2S1	1930.7 [M-H] ⁻	423.4
	F(6)A2G2S1	2076.7 [M-H] ⁻	442.0
	A2G2B	1940.6	414.6
	F(6)A2G2B	2086.7	435.4
	A2G2S2	2221.8 [M-H] ⁻	450.8
	F(6)A2G2S2	2367.8 [M-H] ⁻	475.8
	A3G3	2202.7	435.8
	A4G4	2467.8	469.9

 fucose


 mannose


 galactose

 *N*-acetylglucosamine

 *N*-acetylneuraminic acid

linkages

 α

 β

6
4
3
2

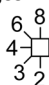


Figure 9. Estimated ^{TW}CCS_{N₂ values of complex N-glycans. Glycan structures, name, and phosphate adduct m/z are presented. The degree of glycan branching is indicated, “A2” (bi-antennary), A3 (tri-antennary), and “A4” (tetra-antennary). The number of terminal galactose follows with “G2” being two galactose, “G3” equal to three, etc. This is similar for the number of sialic acids (“S”). The presence of alpha1–6 linked core fucose is designated as “F(6)” and a bisecting GlcNAc is “B.” Structures are represented using the Oxford system (green circle = mannose, blue square = GlcNAc, yellow diamond = galactose, red diamond with dot (for deoxy) = fucose, purple star = *N*-acetylneuraminic acid (i.e., sialic acid)) [36]}

structures (**m–q**, Scheme 1) are possible from complex glycans lacking galactose and another four (not shown) if galactose is present. Three ATD peaks (Fig. 7, bottom) were found from glycans lacking galactose. The biantennary glycan F(6)A2 yielded a single peak. $\text{Man}_3\text{GlcNAc}_2$, which can only yield ion **m**, gave a single ATD similar to that from F(6)A2. This peak corresponds to structures **n** and/or **o**. The un-galactosylated triantennary glycan, A3, also yielded this peak but, in addition, produced a second which, presumably, could be assigned structure **p**. It was not present in the spectrum of the fucosylated glycan from human α 1-acid glycoprotein which contains the fucose attached to this GlcNAc residue, supporting this structure. The non-glycosylated, tetra-antennary glycan produced peak 2. Antennae containing galactose could not be differentiated by this technique. These results show that some of the ions at m/z 748 have different cross sections but that it was only the un-galactosylated triantennary glycan that appeared to give a unique structure.

These results confirm that fragmentation of branched structures is very heterogeneous due to neutral losses from different arms. Additionally, this is complicated by the possibility of cross-ring fragmentation of either GlcNAcs on the chitobiose core. Furthermore, we do not account for possible gas-phase conformers which is exceedingly difficult to assign especially for deprotonated glycan ions as discussed above. It is equally possible that deprotonated fragments with the same structure adopt different conformers which would lead to alternate drift times and account for the observations described here. Therefore, although negative ion analysis is desirable when performing MS/MS alone for its propensity to generate cross-ring fragmentation, the presence of larger fragments complicates interpreting IM ATD data and efforts should focus on investigating smaller fragment ions.

Conclusions

The combination of CID applied pre-IM yields considerable glycan structural data and through interpreting the spectra of pure, synthetic glycan standards, we can start to understand the gas-phase behavior and, therefore, the potential of IM for glycomics. Here, we have described IM separation of complex type N-glycans as both intact glycan phosphate adducts and of fragments following CID in negative ion mode. These results show that (1) some isomeric structures can be identified by the drift time properties of CID products in cases where IM separation of parent ions fails and (2) the presence of various product ion structures is represented by multiple ATD peaks.

Acknowledgements

W.S. and M.C. gratefully acknowledge a research grant from Against Breast Cancer (www.againstbreastcancer.org; UK Charity 1121258).

References

- Clowers, B.H., Dwivedi, P., Steiner, W.E., Hill Jr., H.H., Bendiak, B.: Separation of sodiated isobaric disaccharides and trisaccharides using electrospray ionization-atmospheric pressure ion mobility-time of flight mass spectrometry. *J. Am. Soc. Mass Spectrom.* **16**, 660–669 (2005)
- Mookherjee, A., Guttman, M.: Bridging the structural gap of glycoproteomics with ion mobility spectrometry. *Curr. Opin. Chem. Biol.* **42**, 86–92 (2017)
- Gray, C.J., Thomas, B., Upton, R., Migas, L.G., Eyers, C.E., Barran, P.E., Flitsch, S.L.: Applications of ion mobility mass spectrometry for high throughput, high resolution glycan analysis. *Biochim. Biophys. Acta.* **1860**, 1688–1709 (2016)
- Zhu, M., Bendiak, B., Clowers, B., Hill Jr., H.H.: Ion mobility-mass spectrometry analysis of isomeric carbohydrate precursor ions. *Anal. Bioanal. Chem.* **394**, 1853–1867 (2009)
- Huang, Y., Dodds, E.D.: Ion mobility studies of carbohydrates as group I adducts: isomer specific collisional cross section dependence on metal ion radius. *Anal. Chem.* **85**, 9728–9735 (2013)
- Harvey, D.J., Crispin, M., Bonomelli, C., Scrivens, J.H.: Ion mobility mass spectrometry for ion recovery and clean-up of MS and MS/MS spectra obtained from low abundance viral samples. *J. Am. Soc. Mass Spectrom.* **26**, 1754–1767 (2015)
- Harvey, D.J., Sobott, F., Crispin, M., Wrobel, A., Bonomelli, C., Vasiljevic, S., Scanlan, C.N., Scarff, C.A., Thalassinou, K., Scrivens, J.H.: Ion mobility mass spectrometry for extracting spectra of N-glycans directly from incubation mixtures following glycan release: application to glycans from engineered glycoforms of intact, folded HIV gp120. *J. Am. Soc. Mass Spectrom.* **22**, 568–581 (2011)
- Fenn, L.S., McLean, J.A.: Structural resolution of carbohydrate positional and structural isomers based on gas-phase ion mobility-mass spectrometry. *Phys. Chem. Chem. Phys.* **13**, 2196–2205 (2011)
- Huang, Y., Dodds, E.D.: Ion-neutral collisional cross sections of carbohydrate isomers as divalent cation adducts and their electron transfer products. *Analyst.* **140**, 6912–6921 (2015)
- Struwe, W.B., Baldauf, C., Hofmann, J., Rudd, P.M., Pagel, K.: Ion mobility separation of deprotonated oligosaccharide isomers—evidence for gas-phase charge migration. *Chem Commun (Camb).* **52**, 12353–12356 (2016)
- Zhu, F., Glover, M.S., Shi, H., Trinidad, J.C., Clemmer, D.E.: Populations of metal-glycan structures influence MS fragmentation patterns. *J. Am. Soc. Mass Spectrom.* **26**, 25–35 (2015)
- Hofmann, J., Hahm, H.S., Seeberger, P.H., Pagel, K.: Identification of carbohydrate anomers using ion mobility-mass spectrometry. *Nature.* **526**, 241–244 (2015)
- Zheng, X., Zhang, X., Schocker, N.S., Renslow, R.S., Orton, D.J., Khamisi, J., Ashmus, R.A., Almeida, I.C., Tang, K., Costello, C.E., Smith, R.D., Michael, K., Baker, E.S.: Enhancing glycan isomer separations with metal ions and positive and negative polarity ion mobility spectrometry-mass spectrometry analyses. *Anal. Bioanal. Chem.* **409**, 467–476 (2017)
- Li, H., Giles, K., Bendiak, B., Kaplan, K., Siems, W.F., Hill Jr., H.H.: Resolving structural isomers of monosaccharide methyl glycosides using drift tube and traveling wave ion mobility mass spectrometry. *Anal. Chem.* **84**, 3231–3239 (2012)
- Pu, Y., Ridgeway, M.E., Glaskin, R.S., Park, M.A., Costello, C.E., Lin, C.: Separation and identification of isomeric glycans by selected accumulation-trapped ion mobility spectrometry-electron activated dissociation tandem mass spectrometry. *Anal. Chem.* **88**, 3440–3443 (2016)
- Harvey, D.J., Abrahams, J.L.: Fragmentation and ion mobility properties of negative ions from N-linked carbohydrates: part 7. Reduced glycans. *Rapid Commun Mass Spectrom.* **30**, 627–634 (2016)
- Hofmann, J., Struwe, W.B., Scarff, C.A., Scrivens, J.H., Harvey, D.J., Pagel, K.: Estimating collision cross sections of negatively charged N-glycans using traveling wave ion mobility-mass spectrometry. *Anal. Chem.* **86**, 10789–10795 (2014)
- Guile, G.R., Rudd, P.M., Wing, D.R., Prime, S.B., Dwek, R.A.: A rapid high-resolution high-performance liquid chromatographic method for separating glycan mixtures and analyzing oligosaccharide profiles. *Anal. Biochem.* **240**, 210–226 (1996)
- Harvey, D.J.: Fragmentation of negative ions from carbohydrates: part 3. Fragmentation of hybrid and complex N-linked glycans. *J. Am. Soc. Mass Spectrom.* **16**, 647–659 (2005)

20. Harvey, D.J.: Fragmentation of negative ions from carbohydrates: part 2. Fragmentation of high-mannose N-linked glycans. *J. Am. Soc. Mass Spectrom.* **16**, 631–646 (2005)
21. Harvey, D.J., Royle, L., Radcliffe, C.M., Rudd, P.M., Dwek, R.A.: Structural and quantitative analysis of N-linked glycans by matrix-assisted laser desorption/ionization and negative ion nanospray mass spectrometry. *Anal. Biochem.* **376**, 44–60 (2008)
22. Gray, C.J., Schindler, B., Migas, L.G., Picmanova, M., Allouche, A.R., Green, A.P., Mandal, S., Motawia, M.S., Sanchez-Perez, R., Bjarnholt, N., Moller, B.L., Rijs, A.M., Barran, P.E., Compagnon, I., Evers, C.E., Flitsch, S.L.: Bottom-up elucidation of glycosidic bond stereochemistry. *Anal. Chem.* **89**, 4540–4549 (2017)
23. Both, P., Green, A.P., Gray, C.J., Sardzik, R., Voglmeir, J., Fontana, C., Austeri, M., Rejzek, M., Richardson, D., Field, R.A., Widmalm, G., Flitsch, S.L., Evers, C.E.: Discrimination of epimeric glycans and glycopeptides using IM-MS and its potential for carbohydrate sequencing. *Nat. Chem.* **6**, 65–74 (2014)
24. Guttman, M., Lee, K.K.: Site-specific mapping of sialic acid linkage isomers by ion mobility spectrometry. *Anal. Chem.* **88**, 5212–5217 (2016)
25. Barroso, A., Gimenez, E., Konijnenberg, A., Sancho, J., Sanz-Nebot, V., Sobott, F.: Evaluation of ion mobility for the separation of glycoconjugate isomers due to different types of sialic acid linkage, at the intact glycoprotein, glycopeptide and glycan level. *J. Proteome.* **173**, 22–31 (2018)
26. Hofmann, J., Stuckmann, A., Crispin, M., Harvey, D.J., Pagel, K., Struwe, W.B.: Identification of lewis and blood group carbohydrate epitopes by ion mobility-tandem-mass spectrometry fingerprinting. *Anal. Chem.* **89**, 2318–2325 (2017)
27. Guile, G.R., Harvey, D.J., O'Donnell, N., Powell, A.K., Hunter, A.P., Zamze, S., Fernandes, D.L., Dwek, R.A., Wing, D.R.: Identification of highly fucosylated N-linked oligosaccharides from the human parotid gland. *Eur. J. Biochem.* **258**, 623–656 (1998)
28. Fournier, T., Medjoubi, N.N., Porquet, D.: Alpha-1-acid glycoprotein. *Biochim. Biophys. Acta.* **1482**, 157–171 (2000)
29. Hernández, H., Robinson, C.V.: Determining the stoichiometry and interactions of macromolecular assemblies from mass spectrometry. *Nat. Protoc.* **2**, 715–726 (2007)
30. Domon, B., Costello, C.E.: A systematic nomenclature for carbohydrate fragmentations in fab-MS spectra of glycoconjugates. *Glycoconj. J.* **5**, 397–409 (1988)
31. Borovcova, L., Hermannova, M., Pauk, V., Simek, M., Havlicek, V., Lemr, K.: Simple area determination of strongly overlapping ion mobility peaks. *Anal. Chim. Acta.* **981**, 71–79 (2017)
32. Thalassinos, K., Grabenauer, M., Slade, S.E., Hilton, G.R., Bowers, M.T., Scrivens, J.H.: Characterization of phosphorylated peptides using traveling wave-based and drift cell ion mobility mass spectrometry. *Anal. Chem.* **81**, 248–254 (2009)
33. Struwe, W.B., Agravat, S., Aoki-Kinoshita, K.F., Campbell, M.P., Costello, C.E., Dell, A., Ten, F., Haslam, S.M., Karlsson, N.G., Khoo, K.H., Kolarich, D., Liu, Y., McBride, R., Novotny, M.V., Packer, N.H., Paulson, J.C., Rapp, E., Ranzinger, R., Rudd, P.M., Smith, D.F., Tiemeyer, M., Wells, L., York, W.S., Zaia, J., Kettner, C.: The minimum information required for a glycomics experiment (MIRAGE) project: sample preparation guidelines for reliable reporting of glycomics datasets. *Glycobiology.* **26**, 907–910 (2016)
34. Kolarich, D., Rapp, E., Struwe, W.B., Haslam, S.M., Zaia, J., McBride, R., Agravat, S., Campbell, M.P., Kato, M., Ranzinger, R., Kettner, C., York, W.S.: The minimum information required for a glycomics experiment (MIRAGE) project: improving the standards for reporting mass spectrometry-based glycoanalytic data. *Mol. Cell. Proteomics.* **12**, 991–995 (2013)
35. Harvey, D.J., Scarff, C.A., Edgeworth, M., Pagel, K., Thalassinos, K., Struwe, W.B., Crispin, M., Scrivens, J.H.: Travelling-wave ion mobility mass spectrometry and negative ion fragmentation of hybrid and complex N-glycans. *Journal of mass spectrometry : JMS.* **51**, 1064–1079 (2016)
36. Harvey, D.J., Merry, A.H., Royle, L., Campbell, M.P., Dwek, R.A., Rudd, P.M.: Proposal for a standard system for drawing structural diagrams of N- and O-linked carbohydrates and related compounds. *Proteomics.* **9**, 3796–3801 (2009)